Turbulent Motion, Mixing, and Kinetics in a Chemical Reactor Configuration

The nature of turbulence and mixing in a reactor used by Toor for kinetic studies was investigated in detail. Simple empirical methods were useful for estimating the decay of the scalar fluctuations. An equation, based on continuity, was used with measured velocities and an improved procedure at the inlet to calculate results that agree well with the kinetic data.

KENNETH N. McKELVEY, HEH-NIEN YIEH, STEPHEN ZAKANYCZ, and ROBERT S. BRODKEY

Department of Chemical Engineering
The Ohio State University
Columbus, Ohio 43210

SCOPE

Our first objective was to establish the concentration and velocity fields without chemical reaction in reactors similar to those used by Vassilatos and Toor (1965) and Mao and Toor (1971) to study chemical reactions under turbulent flow conditions. Their studies and ours combine to furnish the only complete set of data on turbulent mixing with chemical reaction. The reactor configuration had a feed module that separated the two feed streams into many alternating small streams so as to provide a grossly mixed initial condition. The mixing occurred downstream in a pipe that followed the feed module. Our second objective was to use the information on mixing to predict the course of reactions where both the turbulent mixing and kinetics are contributing factors.

One of the most challenging problems facing the reactor designer is that of predicting conversion as a function of position and time in a chemical reactor. This problem is even more difficult if the mixing field is turbulent. The goal is to predict the turbulent field for a given geometry, the mixing from a knowledge of the turbulent field, and the course of chemical reactions from knowledge of the mixing field. There are two extremes in the process. First, for very slow reactions, when chemical rate is the controlling factor, the turbulent mixing is unimportant. Second, for very rapid reactions, the chemical rate is unimportant, and the conversion is controlled by the turbulent mixing. The former can be approached by using residence-time-distribution and kinetic information. The latter is controlled by the turbulent mixing and will be treated in this paper; the main emphasis, however, will be on the problem where both kinetics and mixing must be considered.

The success of earlier studies of turbulence and mixing in a pipeline system (Lee and Brodkey, 1964; Gegner and Brodkey, 1966; Brodkey, 1966; and Nye and Brodkey, 1967a) encouraged us to gather similar results for the reactor designs that had been used to obtain chemical rate data. Hot-film and hot-wire anemometry were used to measure the velocity field, and a light-probe system was used for the concentration field (Lee and Brodkey, 1963; Nye and Brodkey, 1967b). The reactor systems were identical with those of Vassilatos and Toor (1965) and Mao and Toor (1971).

CONCLUSIONS AND SIGNIFICANCE

The flow in the reactors was quite complicated, especially in the region immediately downstream from the injector plane. The measurements in this region depended on the hot-wire location (centered on one of the injector tubes or located between two injector tubes). Beyond the jet coalescence plane the results merged. The mean axial velocity centered on a jet decayed rapidly with distance from the feed module. The velocity measured between two adjacent injector tubes rose rapidly and merged at the coalescence point with that measured on a jet center. After coalescence of the jets, the velocities decayed slowly over the range where reaction would occur. The velocity fluctuations initially rose from a low value associated with the turbulence in the small tube or that associated with the region between two jets. The results merged at the coalescence plane and continued to decrease as expected, but then unexpectedly increased. This nonideal flow is attributed to the formation of a large vortex or separation along the wall near the entrance of the reactor. Results on correlations and spectra were used to compute the characteristic turbulence parameters: velocity macroscale and microscale, low wave number cutoff, and kinetic energy dissipation rate. These are essential for calculating the mixing from a knowledge of the turbulent field. Empirical estimates for the parameters require knowledge of the axial turbulent velocity intensity and a characteristic dimension of the flow system; unfortunately, we do not know which dimension is characteristic for the reactor, so that the estimates made were of uncertain usefulness.

The concentration field was measured with light-probe system, and the fluctuation intensity was found to obey a $(-3/2)$ power law. It is encouraging that this law holds in the nonideal velocity field observed in the reactor as well as in more ideal fields as found by others. The theory for decaying velocity fields could not be used to estimate the scalar decay because of the nonideal decay of the velocity fluctuation as described above. The theory for a stationary velocity field was therefore used to estimate the mixing at specific locations. Even though crude, because of uncertainty of the characteristic dimension, order-of-magnitude or better estimates could be made for the decay of the scalar fluctuations. This is the same theory earlier used by Brodkey (1975) for pipe flow

Correspondence concerning this paper should be addressed to R. S. Brodkey. K. N. McKelvey is with the duPont Company. H.-n. Yieh is with B. F. Goodrich Chemicals Company, and Stephen Zakanycz is with DARPA, Arlington, Virginia.

mixing. The conversion in very rapid reactions is directly related to this decay, and thus, once the mixing is predicted, so is the chemical conversion. The comparison is excellent.

One-dimensional scalar spectra were measured, but much of the spectral energy lay beyond the cutoff frequency of the light probe and could not be detected. Far enough downstream from the feed module a (−1) power law region was observed. The existence of such a region in mixing at large Schmidt numbers has been suggested by Batchelor (1959). Both the concentration and velocity fluctuations were found to be normally distributed.

The prediction of second-order, irreversible chemical reactions where both the kinetics and turbulence are important was studied in some detail. The descriptive equation can be integrated from the inlet (if measured velocity data are available) if one assumes that the velocity and concentration fields are not correlated, that the diffusion term is small, and that mixing is not affected by kinetics (Toor's hypothesis). This latter is adequate for stoichiometric ratios as high as 3.88. The calculated results compare well with the experimental data on the two reactors used by Vassilatos and Toor (1965) and Mao and Toor (1971).

From this work one may conclude that in a well-defined turbulent field, estimates can be made of the expected mixing, and this in turn can be used to predict chemical reaction with simple kinetics. The results are significant for turbulent chemical reactor design.

The studies by Vassilatos and Toor (1965) and Mao and Toor (1971) are important because they are the only ones that treat chemical conversion affected by turbulent mixing in a single system over a wide range of reaction rates. They would be more valuable if the mixing and velocity fields were known. The purpose of this study was to measure the velocity and concentration fields in identical reactors. The second goal was to use the information obtained to predict the course of chemical reactions where both the kinetics and the turbulence must be considered to determine the conversion. Background literature for this work has been reviewed by Brodkey (1975) and Toor (1975). More specific references will be cited as needed.

EXPERIMENTAL

The experimental work consisted in duplicating the reactors used by Toor and his co-workers and measuring the turbulence and mixing under the same conditions as in their experiments. In their work they measured conversions for various reactions at several Reynolds numbers and for different stoichiometric feed ratios. They used dilute aqueous solutions, and in our work we injected a dye-water mixture into water ($D = 2.6 \times 10^{-6}$ cm²/s) to simulate their conditions. Velocity field measurements with a hot-film anemometer in water and a hot-wire anemometer in air were made for identical conditions as used by Vassilatos and Toor (1965). Hot-wire anemometry measurements were also made in air flow for the same conditions studied by Mao and Toor (1971).

The reactor and light probe are shown in Figure 1. The main difference between the two reactors was the number of feed tubes in the 3.18 cm diameter feed module. In the earlier model

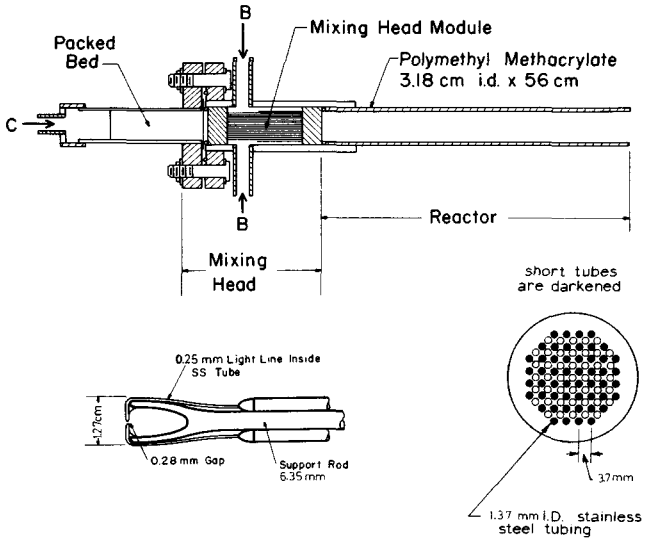

Fig. 1. Mixing reactor, feed module, and light probe.

(A) used by Vassilatos, 97 tubes were used on a square array, and in the later model (B) used by Mao, 188 tubes were used on a close-packed arrangement. For the former, the ratio of closed to open area in the center line region was about 5 and for the latter 2. Thus, the close-packed module should provide considerably less backflow between the jets and a better overall flow pattern. It is important to note that in neither design were fractional tubes used near the outer edge; thus, the entire cross section was not uniformly filled with tubes. Further details of the systems can be found in Vassilatos and Toor (1965), McKelvey (1968), Zakanycz (1971), and Mao and Toor (1971).

For turbulence studies in liquids, it was necessary to minimize temperature change. This was accomplished by recirculating the feed water through a storage tank which contained emersion heaters and a cooling coil. The same source was used to provide the two flows to the mixing head, thereby eliminating the need to maintain two separate temperature controlled streams. It was necessary to filter and degas the water to obtain low drift operation. For concentration studies, water from a large storage tank was mixed with dye from a smaller tank. All the experiments were run at a temperature of 25°C. Variation in water temperature, as measured by a differential thermometer at the exit of the reactor, was less than 0.05°C during the turbulence measurements.

The turbulence measurements in the aqueous system were made by using a Lintronic constant-temperature, hot-film anemometer. An 8 deg. wedge probe was positioned to measure the axial component along the center line. The fluctuating signals were recorded on an Ampex model SP 300 tape recorder at 38.1 cm/s (15 in./s) in both FM mode (D.C. to about 2 500 Hz) and direct mode (40 to 40 000 Hz). The recorded signal was later digitized (Radiation Inc. Model A2, 375 to 40 000 samples/s). The digitized signal was computer processed by autocorrelation techniques and converted to spectrum form.

The more detailed velocity measurements in air were obtained similarly. The inlet air was dried by passing through a silica gel bed, and oil was removed by an oil adsorbent bed. Grove regulators provided flow control. The temperature level could be regulated by heater tapes wrapped around the gas supply pipes. The system was also designed to allow mixing studies of helium and air or of heated and unheated air. To facilitate the extensive measurements made in air, hot-wire sensors were mounted on a three-dimensional traversing assembly. Measurements were made with Thermo-Systems, Inc., miniature hot-wire sensors (90 deg. for u_x and 23 deg. for u_y and u_z) in conjunction with a Thermo-Systems constant-temperature anemometer. Subsequent treatment of the data was similar for both the liquid and air studies.

In the liquid system, the mixing field was measured with a light probe developed by Nye and Brodkey (1967b). Light from a D.C. lamp was focused on the end of a fiber optic line which made up one half of the probe. The other half was a similar return line which conducted the light to the measuring photomultiplier tube. The two ends were separated by a short gap through which the liquid flowed (see Figure 1). The device operated on the Beers' law absorption principle. The electronic instrumentation was essentially the same as used in pre-

vious measurements (Lee and Brodkey, 1963, and Nye and Brodkey, 1967b; details are given by McKelvey, 1968). The earlier light-probe mount was too bulky for use in the reactor, so a smaller mounting configuration was devised. The gap between the two lines was 0.28 mm. The analysis of the concentration signals with regard to linearity and intensity is discussed in the references previously cited and by McKelvey (1968). Because of the extremely efficient mixing in the reactor module, the concentration fluctuations were always a small percentage of the average concentration. Noise problems were far more severe in the present application than in previous uses of the probe. Although useful results were obtained, the use of conductivity measuring devices (Torrest and Ranz, 1969) should be considered for future studies. However, these too have limitations associated with frequency response, range of Schmidt number that can be studied, and size.

DISCUSSION OF RESULTS

Velocity Field

Vassilatos and Toor (1965) selected their reactor (Model A) because they expected that it would generate a scalar field which is homogeneous on a course scale and a velocity field which approximates a convected isotropic field as observed in grid generated turbulence. It was anticipated that, after the coalescence of the jets issuing from the tubes in the feed module, the mean axial velocity distribution would be flat over a considerable distance. The modifications (Model B) made by Mao and Toor (1971) were designed to further improve these flow properties.

Our measurements with a pitot tube indicated that there was, however, strong jetting in the central region of the reaction zone. It was first suspected that this was due to a maldistribution of mass flow through the small tubes of the mixing head. In an attempt to correct this situation, the packed bed in front of the mixing head was added. This and other modifications did not modify the flow pattern. A hydrogen bubble method was used to visualize the flow, and it confirmed the complicated nature of the flow field. Although the spacing between the tubes in the feed modules is uniform, the number of tubes per unit area near the wall is less than near the center of the mixing head module because fractional tubes were not installed near the wall. Thus, the average velocity near the wall was smaller than in the central region. It became clear that a much more complete study of the flow fields following the two feed module designs should be made, and for simplicity these should be made in air rather than water.

Measurements of mean velocity, axial turbulent velocity intensity (u_x'), autocorrelations, and spectra along the center line during water flow in feed module A were made by McKelvey (1968). The Reynolds numbers were 3 600 in the feed module tubes and 15 000 in the reactor. Zakanycz (1971) repeated these measurements in air to demonstrate dynamic similarity and then extended them to include several Reynolds numbers, both feed modules, Reynolds stress terms (u_x', u_y', u_z', $\overline{u_x u_y}$, $\overline{u_x u_z}$), turbulent kinetic energy [$(\frac{1}{2})u_i'^2 = (\frac{1}{2})(u_x'^2 + u_y'^2 + u_z'^2)$], autocorrelations, spectra, and mean and axial fluctuation information as a function of radial position (two radii, one horizontal and one vertical). A number of measurements were made at two locations: one aligned on a feed module inlet tube center and the other located on a line between a cluster of tubes.

Mean and fluctuating axial velocity intensity results will be presented next. These will be followed by an interpretation of what is occurring in the region between inlet jets. A discussion of the nature of the Reynolds stress terms will then be given, and based on this and the previous information, an interpretation of what is occurring along the wall downstream of the entrance will be presented. The section will conclude with the measured turbulence parameters and means of estimating them.

Average Axial Velocity. Figure 2 shows an example of the mean axial velocity along the center line as a function of axial position for feed module A (inlet tube Reynolds number = 3 600). Data obtained by McKelvey (1968) on water flow and the data obtained by Zakanycz (1971) for both alignment on a tube center and between a cluster of tubes are shown. The data of Zakanycz have been scaled by the ratio of kinematic viscosities (18.5 to 1). Adequacy of similarity between the two cases is clear. Air flow results at two lower Reynolds numbers with the same feed module used were similar, but the dip on the between a cluster of tubes curve was not as pronounced at a reactor Reynolds number of 9 400 and did not exist at 5 000. The dip, associated with the region between the jets, will be discussed further after the axial relative intensity is considered. The dip was completely absent at all Reynolds numbers studied in the results obtained on feed module B, which had a very small region between the jets. With the latter feed unit, complete radial traverse measurements were made in both the vertical and horizontal directions to determine the nonideal nature of the flow associated with a wall vortex or separation that will be discussed. Shapes of all of the other radial curves were similar to those shown in Figure 2. The velocities at the feed module face did not vary much across the flow, being about the same high value when located on a tube center and about the same low value when located between a cluster of tubes. Away from the inlet tubes, the values near the wall dropped faster than those measured along the center line. When plotted as a radial traverse, mean axial velocities were reasonably constant over the central 30% of the flow area. Plots of traverses can be found in the appendix of Zakanycz (1971).

Axial Intensity of Turbulence. Along with mean velocity measurements, root-mean-square axial velocity fluctuations

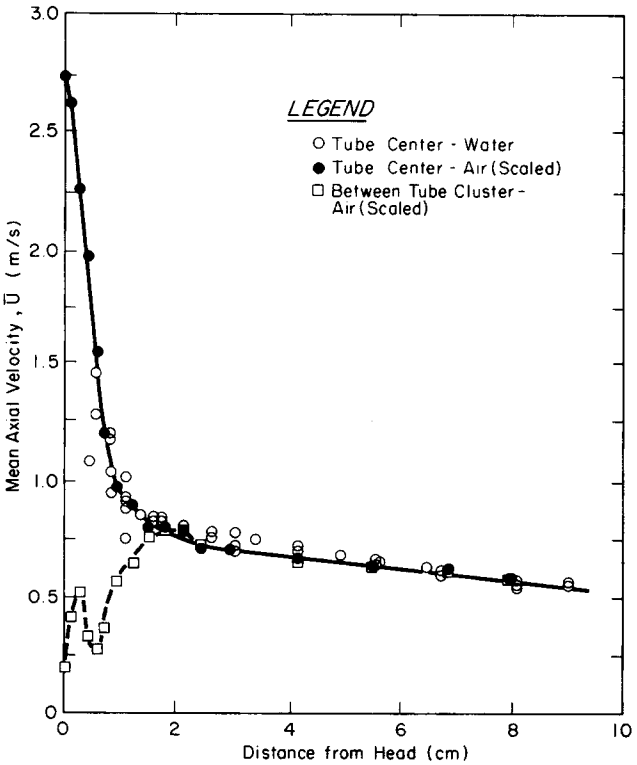

Fig. 2. Average axial velocity along the center line for module A at N_{Re} = 3 600 in inlet tubes and N_{Re} = 15 000 in reactor.

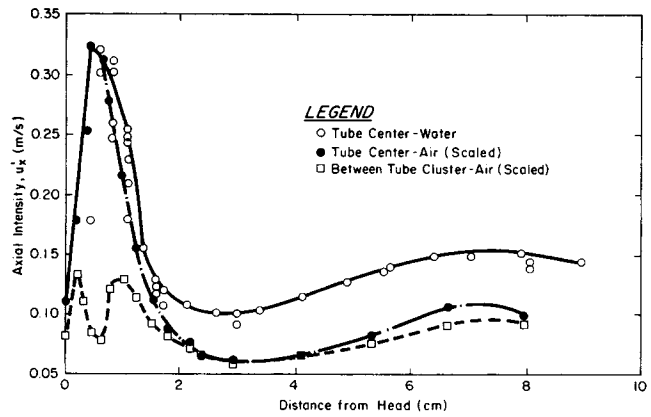

Fig. 3. Axial intensity for same conditions as Figure 2.

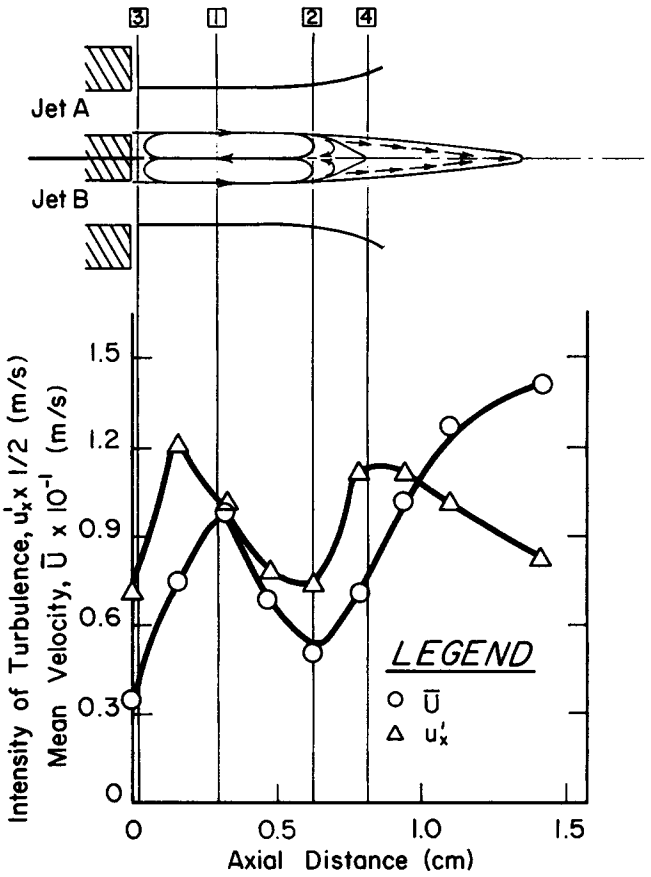

Fig. 4. Flow between jets for same conditions as Figure 2.

(u_x') were measured. Figure 3 provides a comparison for the axial intensity (u_x') of turbulence for the same conditions as shown in Figure 2. Results in air were reproducible, while those obtained in water were less reliable owing to problems associated with drift in the calibrations. Further discussion of this point can be found in Brodkey et al. (1971). Even so, similarity between results is apparent. Results for both feed modules over the range of Reynolds numbers studied were similar. The first dip for the measurements made between a cluster of tubes parallels that observed for the mean axial velocity and, as indicated earlier, is associated with the complex flow in the region between the jets. The intensity is low in this region, but so is the axial velocity; the relative intensity is higher than on tube centers as shown by Zakanycz (1971). A much smaller dip was observed for the feed module used by Mao; recall that no dip was observed in the mean velocity curves for this module.

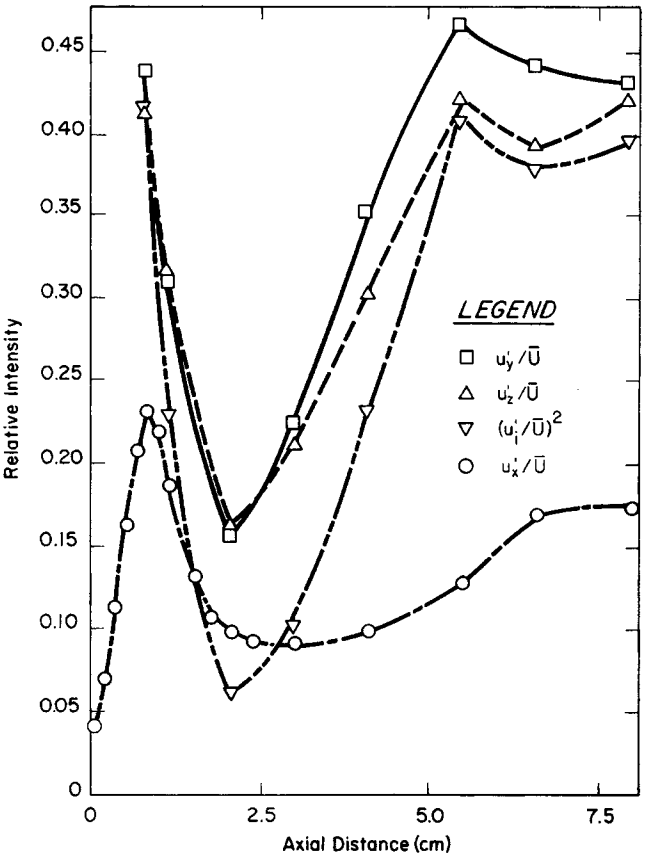

Fig. 5. Relative intensities of all turbulence components for same conditions as Figure 2.

Coalescence of individual jets is characterized by strong interactions producing a great deal of turbulence. As flow continues downstream, there is nothing to sustain this level of turbulent energy, so that it decays rapidly. A second effect, however, soon becomes important. This is a transfer of energy from a vortex that occurs near the wall. The net result is that the axial intensity increases after $x \cong 2.6$ cm. To study this effect, complete radial traverses for the root-mean-square axial velocity intensities are reported in the appendix of Zakanycz (1971).

Flow Region Between Inlet Jets. Mean axial velocity and intensity of turbulence in the region just beyond the inlet tubes can be used to picture the flow in this area. This is an intense mixing region where jets of different composition interact. A backflow apparently exists as is shown in Figure 4. Region (1) is the location where both streams tend to reinforce each other. The position of the hot wire was such that it could be sensitive to this, although, no doubt, some probe mount interference would occur. At region (2) the velocities are opposed and would result in a lower net velocity, and a corresponding lower hot-wire output is observed. Right at the inlet (3) the wall would reduce the velocity. In region (4), the region of jet coalescence, the intensity is high, but so is the mean velocity due to the influence of the jet itself. Needless to say, the picture is qualitative, and flow visualization studies would be needed for a more accurate picture.

Reynolds Stress Terms. To determine if anisotropic flow causes the increase in intensity (Figure 3) after passing through a minimum at 2.6 cm from the inlet, a nominal 30 deg. hot wire was constructed and used to measure horizontal (u_y') and vertical (u_z') intensities of turbulence as well as cross stress terms. The actual angle of the wire as measured with a microscope was 22 deg. 45 min.

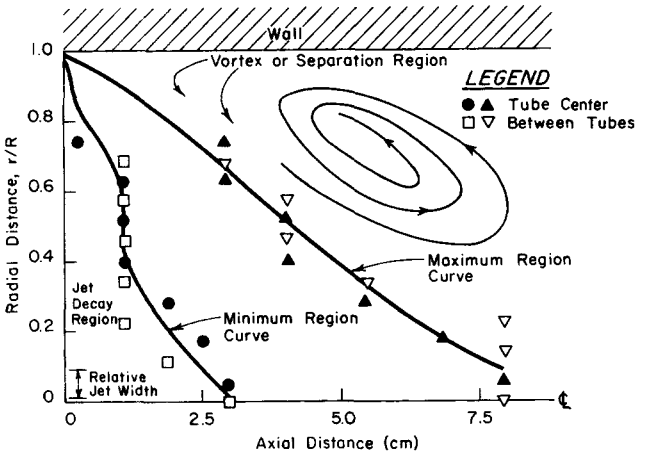

Fig. 6. Wall region flow area map (regions indicated on figure).

Measurements were restricted to the axial center. Data were obtained for both feed modules at an inlet Reynolds number $\approx$ 3 600. Figure 5 shows the results for module A with measurements on an inlet tube center. Other similar results can be found in Zakanycz (1971). The data show that horizontal and vertical relative intensity values are higher than axial intensity values. All relative intensities, including the sum squared, go through a minimum at approximately the same axial distance. If the minimum and subsequent increase were a result of redistribution of u_y' and u_z' energy relative to u_x', then the former should simply decrease, but they too go through the minimum. In fact, the total kinetic energy has the same characteristics, and thus there must be an energy input, not just a redistribution. A different mechanism other than anisotropic conditions is required to explain the increasing values of relative intensities after the minimum is reached.

The values for the cross stress terms (obtained from the difference between two large numbers) were both positive and negative. The values were quite small, so that in this region the cross stress terms are essentially zero as would be expected from the relatively flat velocity profile.

Flow Downstream from the Entrance. Radial traverses of mean velocity and intensity of turbulence were made with the 90 deg. hot wire (for feed module B) in the vertical and horizontal direction for half diameter distances. Vertical and horizontal traversing results, with the hot wire located either on the tube center or between tubes, are presented in a series of figures in the appendix of Zakanycz (1971). Figure 6 summarizes these results and is a plot depicting minimum and maximum values of relative intensity ($u_x'/\overline{U}_x$) as a function of radial and axial distances. It is proposed that the maximum value region be explained by development of either a large vortex or wall separation. A dramatic change is noticed as one moves away from the wall. It is clear that a completely flat root-mean-square velocity profile does not exist in the reactor in the region investigated, since the mean profile was constant over the central 30%.

The Characteristic Parameters of the Turbulent Velocity Field. Autocorrelations, energy spectra, and probability density of the velocity fluctuations were calculated. These describe the velocity fields in the time, frequency, and probability domains, respectively. Details of the computation are given by Brodkey et al. (1971), and examples of all of these can be found for the liquid flow system in McKelvey (1968) and for the air flow work in Zakanycz (1971). To save space, these will not be shown here, but

TABLE 1. SUMMARY OF VELOCITY PARAMETERS FOR FEED MODULE A AND FOR FLOW ON A TUBE CENTER

Position from feed	1.1 cm				3.02 cm				8.10 cm			
r_0 cm	1.1[a]		1.59[b]		1.59							
ν cm^2/s	0.009 (water)		0.167 (air)		0.009		0.167		0.009		0.167	
$\overline{U}_x$ cm/s	89.4		1,921		74.7		1,515		57.4		1,046	
u_x' cm/s	25.4		300		9.33		145		13.8		235	
	Exp.	Est.	Exp.	Est.	Exp.	Est.	Exp.	Est.	Exp.	Est.	Exp.	Est.
λ cm	0 042	0.036	0.091	0.046	0.072	0.088	0.079	0.130	0.059	0.110	0.062	
L_f cm	0.18	0.41	0.21	0.41	0.60	0.32	0.60	0.51	0 60	0.53	0.60	
ϵ cm^2/s^3	4.7 $\times$ 10^4	6.6 $\times$ 10^4	1.4 $\times$ 10^3	2.7 $\times$ 10^7	2.2 $\times$ 10^3	10.8 $\times$ 10^7	6.39 $\times$ 10^6	8.4 $\times$ 10^6	1.1 $\times$ 10^3	7.3 $\times$ 10^3	1.09 $\times$ 10^7	3.6 $\times$ 10^7
k_0 cm^{-1}	1.74	1.82	0.54	1.82	1.10	1.26	1.14	1.26	0.24	1.26	0.46	1.26

[a] Coalescence length.
[b] Radius of reactor.

	Experiment	Estimation
λ^2	$= (u_x'^2/2) \int_0^\infty k^2 \phi(k)\, dk$	$\cong 3.41\ \nu\ r_0/u_x'$
L_f	$= (\pi/u_x'^2)\ \phi(0)$	$\cong (3/8)\ r_0$
ϵ	$= 15\ \nu\ u_x'^2/\lambda^2$	$\cong 4.40\ u_x'^3/r_0$
k_0	$= (2/3)^{3/2}\ \epsilon/u_x'^3$	$\cong 2/r_0$

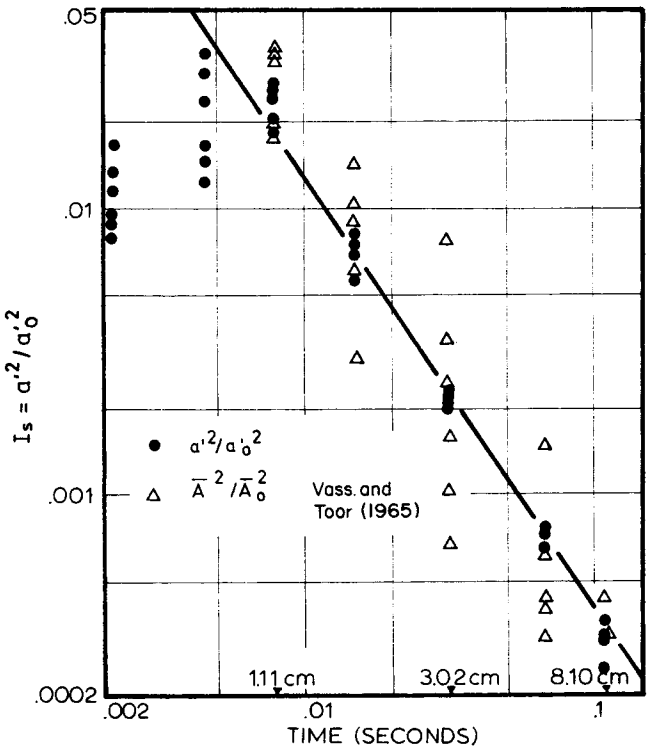

Fig. 7. Decay of the concentration fluctuations.

some brief comments are in order. A low frequency oscillation existed in the autocorrelations and was probably due to the wall effect which produced a repetitive structure of approximately one size. The same effect could be seen, as expected, in the spectra. Preferential formation of eddies of a specific size by the wall influence was responsible for a maximum in the spectra in the range of 10 to 100 Hz. Probability distributions were nearly normal.

Of importance in estimating mixing are the parameters that are descriptive of the turbulence and are obtained from the correlations and spectra. The equations for these parameters, the microscale (λ), macroscale (L_f), low wave number cutoff (k_0), and the kinetic energy dissipation (ϵ), are in Table 1. Means of obtaining these and results for pipe flow have been discussed by Brodkey et al. (1971) and reviewed by Brodkey (1975). Details can also be found in the theses upon which this work is based. Also presented in the references cited are a series of empirical estimates for these parameters. These estimates require only a knowledge of the axial turbulent velocity intensity and a characteristic length scale for the geometry, such as the radius of a pipe. Near the feed module, the coalescence length (1.1 cm) was selected as the characteristic length for best agreement. Comparisons are satisfactory (all within a factor of 5), especially when one considers the large difference in kinetic energy dissipation between the water and air flows. At the position where the axial turbulent velocity was a minimum (about 3 cm from the feed module), the characteristic length was taken as reactor tube radius, as would be done for pipe flow. The comparisons are quite good. The same characteristic length should still apply further downstream, and at a position of 8.10 cm the results are also quite good. The only major difference is the dissipation for the water flow. Further similar results at other positions and with the other feed modules can be found in Zakanycz (1971). One should recognize that the various relations used for the estimates are for isotropic turbulence, strictly speaking, and errors may also reflect deviation from such conditions.

Concentration Field and Fast Reaction

Turbulence measurements were made to understand the nature of the flow in the reactor and to provide information necessary to predict the course of mixing. Mixing and its prediction will be discussed in this section. In addition, if a chemical reaction is very fast, then mixing can be easily related to fractional conversion in the reaction. The case where the conversion depends on both the kinetics and the degree of mixing will be treated in the next section.

Measurements of the scalar field were much more difficult to make than in previous studies of mixing in pipe flows with the light probe because the reactor is a much more effective mixer. As a result, the magnitude of concentration fluctuations was considerably smaller ($a'/\bar{A} = 0.08$) than that encountered by Nye and Brodkey (1967a) ($a'/\bar{A} = 0.5$) or by Lee and Brodkey (1964) ($a'/\bar{A} = 0.15$). Because smaller concentration fluctuations were being measured, signal-to-noise ratio was lower than previously encountered, and analysis of results was more difficult.

Decay of the Concentration Fluctuations. The most important single statistic of the scalar field is I_s, Figure 7. Downstream of the coalescence plane, the decay is well represented by

$$I_s = \frac{a'^2}{a_0'^2} = (1.28 \times 10^{-5})t^{-3/2} \qquad (1)$$

with a' being the rms concentration fluctuation, a_0' being the initial value of this, and time in seconds. The $(-3/2)$ power law dependency has previously been observed by Gibson and Schwarz (1963) and by Keeler et al. (1965) and predicted theoretically by Hinze (1959). These results were obtained in velocity fields which were approximately isotropic. Torrest and Ranz (1970) measured the concentration decay in a system somewhat similar to the one used here and observed a decay that fell between a (-1) and $(-3/2)$ power law dependency. It may be, therefore, that decay of passive scalar fields is rather insensitive to many details of decay of the velocity field and that scalar fields associated with decaying anisotropic velocity fields approximate the $-3/2$ law.

The time used in plotting Figure 7 is the average time required for a fluid element to flow from the head to the position x at which the measurements were taken. Therefore

$$t = \int_0^x \frac{1}{U_x}\, dx$$

The method of calculating a_0' should be mentioned. The value a_0' should be the average of the concentration fluctuations at the downstream face of the head. Since concentrations of jets leaving the head were not known with great accuracy, a_0' was selected as the value which yielded best agreement with Vassilatos' data. Values thus calculated were within experimental error of area averaged values. In any case, an improper choice of a_0' would merely add a constant to the data on a log-log plot and would not alter the shape of the decay curve.

One-Dimensional Scalar Spectrum. Calculation of the one-dimensional scalar spectrum, defined as

$$\varphi_s(k) = \frac{2}{\pi}\int_0^\infty a'^2 f_s(r_x) \cos kr_x\, dr_x \qquad (2)$$

where $f_s(r_x)$ is the correlation of the concentration fluctuations, paralleled the calculation of the velocity spectrum. To save space, details will not be presented here. Calcula-

TABLE 2. SUMMARY OF SCALAR PARAMETERS

Position from head, cm		1.1	3.02	8.10
λ_s cm		0.00041	0.00081	0.0015
L_s cm		0.015	0.020	0.046
$\epsilon_s/a_0'^2$ s^{-1}		3.75	0.103	0.00437
$k_{0,s}$ cm^{-1}		18.9	13.5	1.91
τ s (exp.)		0.0044	0.027	0.067
τ s (est.)	(1)	0.024	0.095	0.063
	(2)	0.0042	0.015	

$\lambda_s^2 = -12\,Da'^2/(da'^2/dt)$
$L_s = \pi\,\phi_s(0)/2a'^2$
$\epsilon_s = -da'^2/dt$
$k_{0,s}^{2/3} = (3/2)\,\epsilon_s/a'\epsilon^{1/3}$
Experimental value of τ
$\tau = -t/\ln I_s = -t/\ln(a'^2/a_0'^2)$
Estimated value of τ
see text for explanation of (1) and (2)

tion procedures can be found in McKelvey (1968); results are given in Figure 8.

Although the true spectra extend to much higher frequencies than shown in Figure 8, they were, unfortunately, attenuated at high frequencies by the finite size of the light probe. Much of the spectrum which is above the frequency range of the light probe is both interesting and important from the point of view of chemical reactions. Overall shapes of the spectra are typical of those previously measured in concentration fields. A primary difference between the spectra at the different positions is the decrease in area under the spectra, which equals a'. Characteristically, a larger percentage of a' is lost at high frequencies than at low frequencies because the dissipation preferentially favors high frequencies.

According to Batchelor (1959), and as shown by Nye and Brodkey (1967a) and by Grant et al. (1968), the scalar spectrum should show a -1 region for large Schmidt number experiments. Since the scalar eddies enter this reactor as large elements, it should take a finite amount of time for the velocity field to break these elements down to a small size and for the equilibrium suggested by Batchelor to develop. Time required for a scalar eddy of wave number $(\epsilon/\nu^3)^{1/4}$ to be deformed by the straining process into one of wave number $(\epsilon/\nu D^2)^{1/4}$ is, according to Batchelor

$$T = -\frac{1}{\gamma}\ln(N_{Sc}) \quad \text{with} \quad \gamma = -0.5(\epsilon/\nu)^{1/2}$$

where γ is the rate of strain. These times for the positions 1.10, 3.02, and 8.10 cm from the head are 0.0065, 0.0386, and 0.0375 s. Average times required for the fluid to flow from the head to these positions are 0.007, 0.032, and 0.11 s. Probably the only position for which the -1 range had time to fully develop was the last one, $x = 8.10$ cm, and this position does exhibit about one decade of -1 range.

Probability Density of the Scalar Fluctuations. In addition to the frequency and time domains, the scalar field can be represented in a probability domain. Probability density of the concentration fluctuations at various positions can be found in McKelvey (1968). As might be expected, the distribution is essentially normal. One of the assumptions of Toor's (1962) theory for rapid reactions is that concentration fluctuations are normally distributed, and it appears that this assumption is reasonable.

Characteristics Parameters of the Scalar Field. Values of the scalar macroscale (L_s), microscale (λ_s), dissipation (ϵ_s), $k_{0,s}$, and time constant of mixing (τ) are summarized in Table 2 along with equations used. The decay rate da'^2/dt is determined from the data. Details can be found in McKelvey (1968). The estimation of the time constant

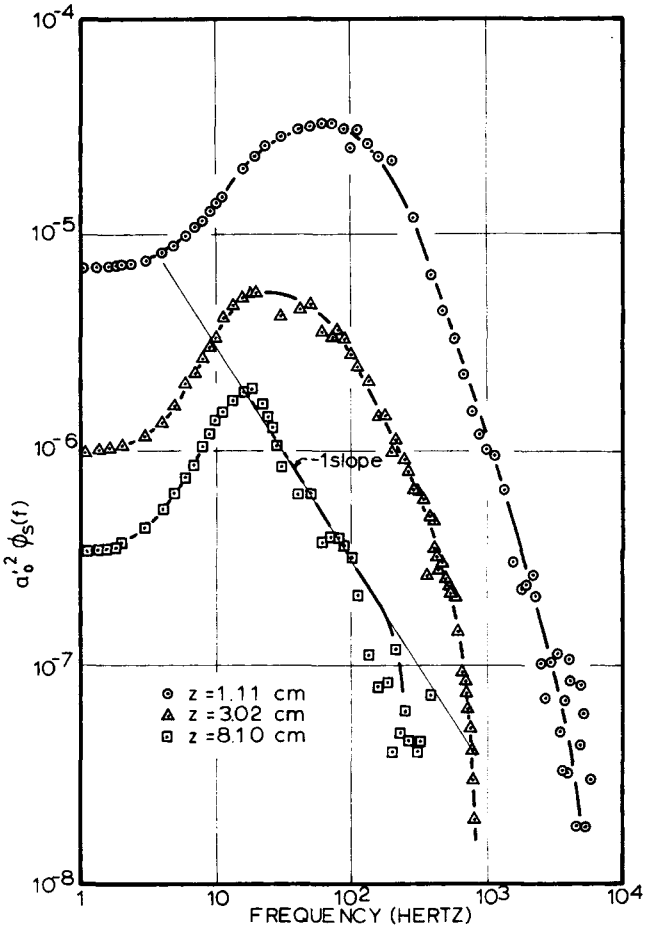

Fig. 8. One-dimensional concentration spectrum.

of mixing needs further clarification. The basic equation comes from the analysis by Corrsin (1964). For low Schmidt numbers

$$\tau = \lambda_s^2/12D = \left(\frac{5}{\pi}\right)^{2/3}\frac{2}{(3 - N_{Sc}^2)}\left(\frac{L_s^2}{\epsilon}\right)^{1/3} \qquad (3)$$

and for high Schmidt numbers

$$\tau = \lambda_s^2/12D = \frac{1}{2}\left[3\left(\frac{5}{\pi}\right)^{2/3}\left(\frac{L_s^2}{\epsilon}\right)^{1/3} + \left(\frac{\nu}{\epsilon}\right)^{1/2}\ln N_{Sc}\right] \qquad (4)$$

In the equations, ϵ is the estimated from the equation given in Table 1 and the term

$$\left(\frac{5}{\pi}\right)^{2/3}\left(\frac{L_s^2}{\epsilon}\right)^{1/3} = 0.341\,r_0/u_x' \qquad (5)$$

first given by Brodkey (1966). The entire procedure as well as a number of examples from pipe flow and mixing tanks can be found in Brodkey (1975). The first estimate of the time constant at the first two positions is based on using r_0 as used for the turbulence. The estimates differ by a factor of 5 or so. However, the characteristic length associated with the mixing does not have to be the same as for turbulence. In the region near the head, the scalar scale can be taken as the expanded jet radius (0.132 cm) rather than the coalescence length (1.1 cm). If this value is used, the second improved estimate is obtained. Such an assumption should be best at the coalescence point (as is observed in Table 2), where the jets have filled the cross-sectional area. The assumption should become pro-

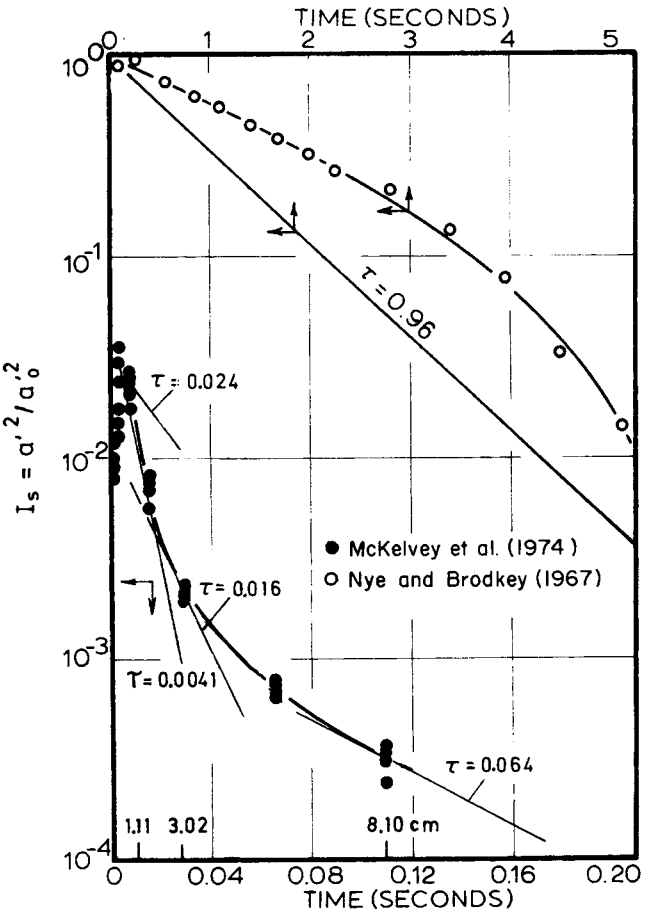

Fig. 9. Comparison with theory for mixing module A and pipe flow data.

gressively worse with distance downstream. At the 3.02 cm position, the estimate is still adequate but certainly not as good as at the coalescence point. The turbulence scale used here was 1.59 cm, the tube radius. As the flow continues downstream, the scale would rise from the expanded jet radius to that of the turbulent field. At the 8.10 cm position, the gross mixing has proceeded to the point where the mixing and turbulent scales are of the same order, so that the characteristic length for both is the pipe radius (1.59 cm). In all cases the normally used characteristic length was retained for the estimate of ϵ as given in Table 1.

The predicted time constants at specific points are further compared to the measurements in Figure 9. A forward integration in time with knowledge of the variation of the time constant of mixing should allow prediction of the entire decay curve. The data of Nye and Brodkey (1967a) for the decay along the center line of a pipe flow are shown for comparison. The faster mixing in the multijet reactor is quite apparent.

Fast Chemical Reaction. One main purpose of our work was to demonstrate the equivalence of the mixing results in the reactor, and the very fast reaction results in the identical geometry as measured by Vassilatos and Toor (1965). The suggested equivalence is a result of the theory of Toor (1962), which is a powerful tool for mixing studies. The only direct test of Toor's work is that by Keeler et al. (1965), who measured both the mixing and fast reaction in the wake of a grid over a range of stoichiometric feed ratios. The effect of stoichiometry in the theory was checked also by Vassilatos and Toor (1965) by first assuming that mixing and very fast reaction results were equivalent for a stoichiometry of unity and then predicting the reaction at other stoichiometric ratios. Thus, all that remains is to show the equivalence of the mixing to the reaction under stoichiometric conditions. Torrest and Ranz (1970) made similar mixing studies, but their flow geometry was not identical to the reactor system used here. To demonstrate the equivalence from this work, Vassilatos' data, in the form of I_s, for very rapid reactions are shown in Figure 9 along with the mixing data without reaction. The intensity of segregation is simply calculated from the fraction conversion (F) by

$$I_s = (1 - F)^2 \tag{6}$$

The agreement is excellent for all times after the coalescence plane, and since Toor's theory does not apply to coarse nonhomogeneous fields, agreement could not be expected before this position. In addition, Toor used an area averaging across the reactor for his averages; in this study time averages were used. These two would be equal only after the coalescence plane. The initial mixing condition was also a problem in the Keeler et al. (1965) work.

One final comparison is possible. It is one that is extremely important since it involves gas mixing as measured by Ajmera (1969), by means of the fast chemical reaction between ozone and nitric oxide. For reaction close to stoichiometric conditions and for a coaxial injector pipe reactor, similar to our pipe system we studied earlier, Ajmera measured fraction conversion along the center line which can be easily translated into I_s. The pipe was a 0.317 cm I.D. tube, 11.43 cm long. No turbulence parameters are available, but the literature data summarized by Brodkey et al. (1971) can be used. The Reynolds number is known, so that the friction factor or U*, the friction velocity, can be determined. From this, u_x' can be estimated, since at the center line

$$u_x' = 1.2\,U^* = 1.2\,\overline{U}_x\sqrt{f/2} \tag{7}$$

By using Equations (3), (5), and the equation for ϵ in Table 1, estimates can be made and compared to experimental results, one example of which is shown in Figure 10. Note that Equation (3) is used rather than Equation (4), since this is a low Schmidt number system. For three different Reynolds numbers, the checks were within 10%. Further details can be found in Zakanycz (1971).

The results for mixing and its prediction in a variety of geometries have been recently reviewed by Brodkey (1975). It is interesting to note the range of time constants predicted and compared to experiments. The slow mixing at the center line of a pipe is characterized by a mixing time constant of about 1 s (see Figure 12). For stirred tank mixing, the constant was about 0.02 s close to the impeller and 0.2 s away from the impeller. In this work, near the inlet from the feed module, the constant was 0.0044 s, and away from the head it was 0.067 s. For the gas reaction in a small pipe, the values ranged from 2×10^{-4} to 8×10^{-4} s. Nearly a 10 000 fold range in mixing times is adequately estimated, if one has some idea as to the proper value of r_0 to be used.

Chemical Reaction

In the Scope, the overall goal of this research was outlined. In earlier sections, the turbulence in a specific reactor, the mixing and its dependency upon the turbulent field, and the relation of the mixing to very rapid chemical reactions were all discussed in some detail. The problem in which both mixing and chemical kinetics are important contributors to determining the overall reaction rate remains to be discussed. Data on such reactions have been obtained by Vassilatos and Toor (1965) and Mao and Toor (1971) on the reactor configurations considered here.

Most of the theory has been developed by Toor. In the next section, the theory will be treated. The final section will compare theory with experimental results.

Theory. The first theories to treat the second order intermediate reaction rate case were based on phenomenological models: Kattan and Adler (1967), Harris and Srivastava (1968), Mao and Toor (1970), Rao and Dunn (1970), and Rao and Edwards (1971) are examples. These and other models have been recently reviewed by Patterson (1975). Phenomenological models can prove useful in practice, but they are models designed to fit overall data and cannot reveal much insight into the mechanism occurring. Thus they will not be considered further here.

A more fundamental approach for the second-order reaction between species A and B [$A + nB \rightarrow (n+1)P$] is to use the mass balance equation for an individual species A:

$$\frac{\partial A}{\partial t} + (\mathbf{U}\cdot\nabla)A = D\nabla^2 A - kAB \tag{8}$$

where A and B are the concentration fractions of species A and B and D is assumed constant. The system is assumed incompressible and isothermal, and the scalar field has no effect on the velocity field. The velocity and concentration can be separated into average and fluctuating parts. When these are substituted into Equation (8), the resulting equation can be averaged to give

$$\frac{\partial \bar{A}}{\partial t} + (\bar{\mathbf{U}}\cdot\nabla)\bar{A} + (\nabla\cdot\overline{\mathbf{u}a}) = D\nabla^2\bar{A} - k(\bar{A}\bar{B} + \overline{ab}) \tag{9}$$

For a one-dimensional reactor, Equation (9) reduces to

$$\frac{\partial \bar{A}}{\partial t} + \bar{U}_x\frac{\partial \bar{A}}{\partial x} + \frac{\partial\, \overline{u_x a}}{\partial x} = D\frac{\partial^2 \bar{A}}{\partial x^2} - k(\bar{A}\bar{B} + \overline{ab}) \tag{10}$$

where x is taken as the axial direction and D, assumed independent of A, is the mutual diffusion coefficient of a mixture of component A and solvent. At steady state without reaction, Equation (10) reduces to

$$\frac{d\,\overline{u_x a}}{dx} = 0 \quad \text{or} \quad \overline{u_x a} = \text{constant} \tag{11}$$

Equation (11) must be true everywhere. When the mixing is completed at the end, the concentration fluctuations become zero, which means

$$\overline{u_x a} = 0 \tag{12}$$

everywhere. This implies that the velocity and concentration fluctuations are not correlated throughout the reactor during mixing, and it is doubtful that they will become correlated when reaction is imposed. Recently, O'Brien (1969) proposed the same statistical independence hypothesis for a decaying single specie reaction in homogeneous turbulence and concluded that the principles which he developed can also be applied to second-order-reactions.

If the flow is two dimensional, Equation (12) will not necessarily be valid. For example, in the pipe flow experiments of Lee and Brodkey (1964), dye was introduced into the reactor by a single tube located at the center of the pipe. Neglect of the radial variation in Equation (9) and the justification following Equation (11) are not valid because the dye diffuses both along and across the pipe; the time average concentration $\bar{A}$ will not be constant throughout the pipe. It may be, however, that such terms

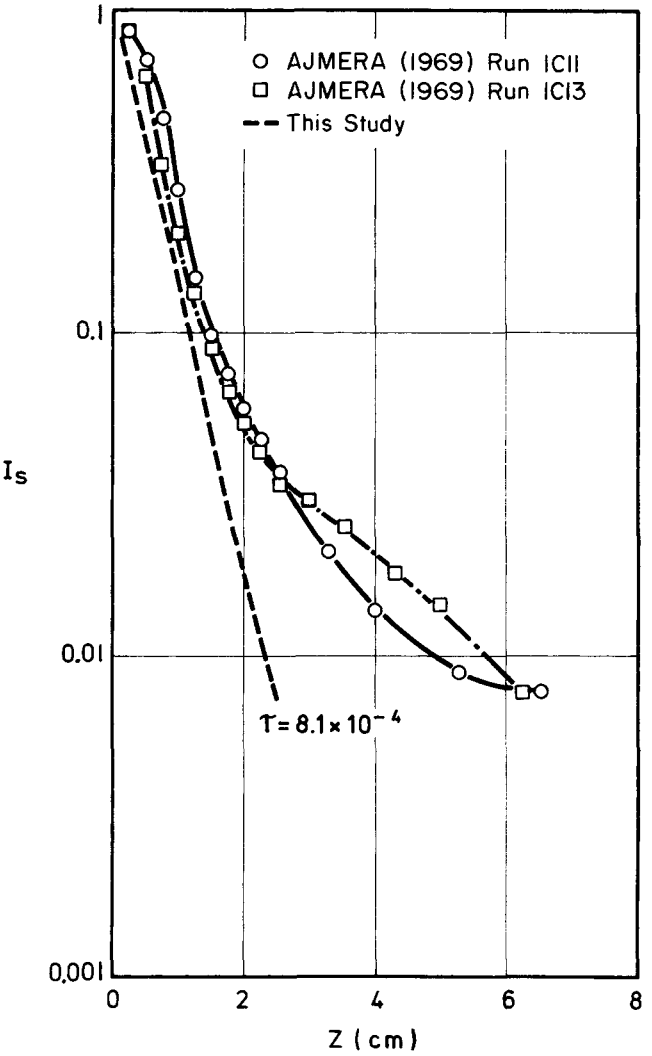

Fig. 10. Comparison between observed and estimated mixing for gas system.

are negligible if not zero. Lee (1962) computed $\overline{u_x a}$ for his single central injector system. One can estimate from continuity that $\bar{U}_x(\partial\bar{A}/\partial x)$ is of the order of $\partial\,\overline{u_x a}/\partial y$. $\partial\,\overline{u_x a}/\partial x$ can also be determined at the location. The variation $\partial\,\overline{u_x a}/\partial y$ or $\bar{U}_x(\partial\bar{A}/\partial x)$ in Lee's case was more than an order of magnitude (30 to 40 times) greater than $\partial\,\overline{u_x a}/\partial x$. Thus in this case the term, although not zero, is quite small. It should be emphasized that usually such measurements are restricted to the center line where the mixing is the slowest in terms of the convected distance (high velocity). Here, of course, owing to symmetry, $\overline{u_x a} = 0$ and $\partial\,\overline{u_x a}/\partial x = 0$, but $\bar{U}_x(\partial\bar{A}/\partial x)$ is large.

For the one-dimensional reactor, at steady state, Equation (10) reduces to

$$\bar{U}_x\frac{d\bar{A}}{dx} = D\frac{d^2\bar{A}}{dx^2} - k(\bar{A}\bar{B} + \overline{ab}) \tag{13}$$

The axial change in $\bar{A}$ still cannot be determined since $\overline{ab}$ is unknown; however, if it can be estimated, Equation (13) could be numerically integrated. Toor (1969) showed that $\overline{ab}$ was the same for very slow reactions and stoichiometric very rapid second-order reactions. The latter had already been shown to be equivalent to pure mixing. With this as background, Toor hypothesized that $\overline{ab}$ was

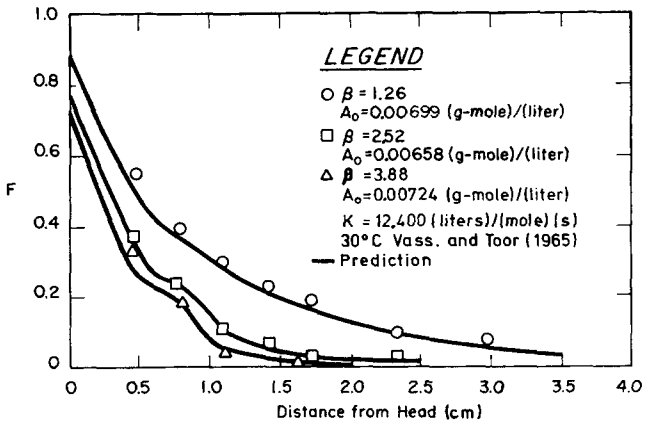

Fig. 11. Comparison between observed and estimated conversion for intermediate rate reaction studied by Vassilatos and Toor.

"independent of the speed of the reaction when the reactants are fed in stoichiometric proportion." He pointed out that this could not be exactly true for nonstoichiometric mixtures. Yieh (1970) attempted to prove the hypothesis by showing that the kinetic term in the equation for $\overline{ab}$ was zero for any reaction level. This could only be done for the unlikely assumption that the products are evenly distributed everywhere. As Toor indicated, it can be shown that this term is zero for stoichiometric very rapid second-order reaction. Under these conditions, $a = -b$ everywhere. For details of this, one can refer to the thesis cited.

To integrate Equation (13) numerically, it is expressed in terms of more convenient variables:

$$\frac{dF}{dx} = \frac{D}{U_x}\frac{d^2F}{dx^2} - \left(\frac{k\,n\,\overline{A}_0\,\beta}{U_x}\right)\left[\frac{F}{\beta}(\beta - 1 + F) - I_s\right] \tag{14}$$

where F = fraction converted $= \overline{A}/\overline{A}_0$

β = stoichiometric ratio $= \overline{B}/n\,\overline{A}_0$

I_s = intensity of segregation $= -\overline{ab}/\overline{A}_0\overline{B}_0 = a'^2/a_0'^2$

In using I_s, it is assumed that $\overline{ab}$ can be determined from mixing with varying β (Toor's hypothesis that $a = -b$).

Comparison of Theory and Experiments. Mao and Toor (1971) integrated Equation (14) and compared the results with experiments. The integration was done by using (1) $D = 0$, (2) $\overline{U}_x$ as the bulk average velocity in the reactor, (3) I_s from very rapid reaction data, and (4) an initial perfect mixing region preceding the region where Equation (14) would apply. Independently, Yieh (1970) integrated the equation, but with fewer assumptions. It is easy to show that the first assumption is adequate. It is known that the bulk average velocity in the reactor is greatly different than the varying axial velocity along the center line (see Figure 2); thus the actual measured variable velocity was used here. The third assumption is the hypothesis above and was used here. The final assumption is phenomenological in nature and made to solve the equation. It would not be needed if the proper boundary condition at the inlet and the actual axial velocities are used.

Equation (14) was integrated by using a fourth-order Runge-Kutta method. The velocity measurements used were made in air and scaled to the temperature conditions actually used to measure the kinetics. Both the axial mean velocities measured at the center of the jetting stream and between jetting streams were used in the calculation. An example was given previously, and details of all of the measurements can be found in Zakanycz (1971). The values of I_s used were taken from the fast reaction results that can be found in Figure 2 of Vassilatos and Toor (1965) and Figure 1 of Mao and Toor (1971). The former are identical to the directly measured mixing results as shown in Figure 7. In this case, the data in the head region were not measured, and the calculations are based on extrapolation to the head ($x = 0$). Both the velocity and I_s were first fitted with a second-order equation by using three adjacent experimental points and then were interpolated for any desired distance. The integration was made from $x = 0$ to 4.06 cm because most of the results reported were in this range. The initial condition was set as $F = 1$ (at $x = 0$), and increments in Δx were taken as 0.0254 cm. From preliminary calculations, the difference between results for F obtained by taking Δx as 0.00254 cm and those using 0.0254 cm were less than 0.001. Therefore, the increment size of 0.0254 cm was used for all the calculations. The value of n for all the intermediate rates of reaction is 2.

It may be well to emphasize once again that the calculation using Equation (14) in this work uses actual measurements for the velocity and measured values of I_s. Everything is defined, and the course of F vs. distance from the reactor head is computed directly. There are no phenomenological models or assumptions such as a preliminary ideal mixer step as Mao and Toor required. Thus this work is a more stringent test of the hypothesis made by Toor and possible extension to larger values of β as Mao and Toor suggested.

Figure 11 shows three of five experiments performed by using feed module A. The stoichiometric ratio varied from 1.26 to 3.88. The remaining comparisons were just as adequate and can be found in Yieh (1970). The reason that the velocity between the jets gives a better predicted result is that at the entrance of the reactor, the ratio of nonflow to flow area is 3.63 for Vassilatos' reactor; therefore the axial mean velocities across most of the reactor head were closer to the axial mean velocity taken between jets than that measured on the center of a jet. The two axial mean velocities represent two limits. The experimental results should lie between the predicted results which were based on these two limits and should be closer to that between the jets, as they were. Patterson (1975) in using the same data in a model simulation found the same effect.

Mao and Toor (1971) attempted to use Equation (14) with their assumptions cited previously to predict the data obtained by Vassilatos and Toor (1965). They reported the predictions were relatively poor at lower values of β and good at the higher values. The failure can be attributed in part to use of bulk average velocity rather than true axial velocity. As shown by Yieh (1970), the differences in using the velocity on a tube center and between the jets is considerable. Thus, one would expect difficulty in using the initial ideal mixing region to compensate for the use of a constant value for the velocity throughout the calculation. The experimental results were also compared with some phenomenological models by Mao and Toor (1970) and by Yieh (1970). These comparisons can contribute little to our understanding of the mechanism and will not be discussed further here.

The experiments reported by Mao and Toor (1971) on the 188 tube feed module are expected to be considerably more reliable than those of Vassilatos and Toor (1965). Our calculation procedure was identical to that just described, and several of the results are shown in Figure 12. The remaining comparisons can be found in Yieh (1970). For these data, the procedure and assumptions used by Mao and Toor are adequate, and they report excellent

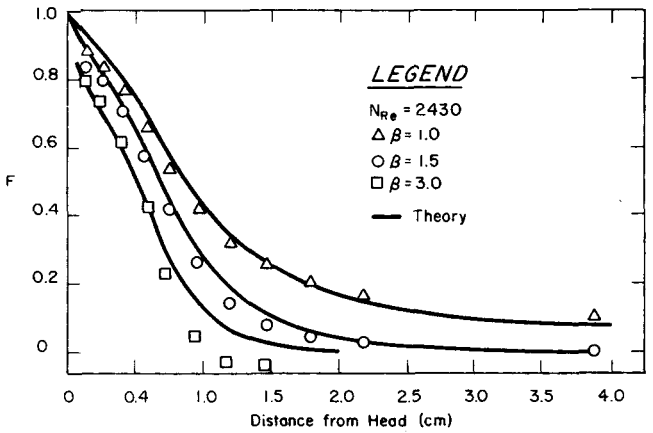

Fig. 12. Comparison between observed and estimated conversion for intermediate rate reaction studied by Mao and Toor.

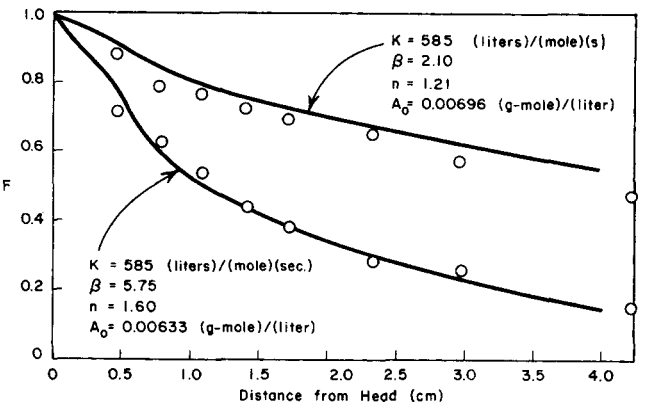

Fig. 13. Comparison between observed and estimated conversion for slow rate reaction studied by Vassilatos and Toor.

checks over the same range of $\beta \leq 3$. We should note that if one attempts our calculation with the bulk average velocity rather than the actual velocity, the results are unsatisfactory. One must use the actual velocity or the modifications by Mao of introducing the ideal mixer step. Thus, it appears that the ideal mixer step compensated for the use of the incorrect velocity.

The overall prediction is not perfect for high conversion ($\beta = 3$). The deviation between the prediction and experiment is large when the reaction is nearly complete. This, however, must be blamed on the data, since the last two points are negative, that is, greater than 100% conversion.

The difference in the prediction between using the velocity as measured in or between the jets is much smaller for Mao's work than for Vassilatos'. This is a direct consequence of the increased number of jets in Mao's system, which corresponds to an increased flow area. The calculated results are affected by a combination of variables: k, A_0, n, β, $\overline{U}_x$, and I_s. The major factor in Vassilatos' case is that most of the mixing was completed in the head region; that is, the values of I_s were lower, and the coalescent point of the jets was farther from the head than in Mao's experiment. This must also be in part the reason why Vassilatos' experimental data were more scattered than Mao's.

In addition to the intermediate rate reaction measurements, Vassilatos and Toor (1965) measured relatively slow reactions. They were able to predict the experimental results for the slowest rate by assuming homogeneity. They were unsuccessful in predicting the somewhat faster reaction rate case by a similar assumption. Figure 13 presents some of the computed results for this case. Again, the complete results can be found in Yieh (1970). The velocity used for this calculation was the one measured between the jets, since for the intermediate rate reaction it was this velocity which provided the good fit. The value of n, which varies from 1 to 2, depends on the relative concentrations of ammonia and carbon dioxide. In spite of the uncertainty in n, the theory adequately predicts the slow reaction results.

ACKNOWLEDGMENT

The authors wish to thank the National Science Foundation and office of Scientific Research/Air Force Institute of Technology for their support of our turbulent mixing studies. Dr. A. Rao as well as Mr. M. Kukla offered considerable help during the course of the experimentation.

NOTATION

$\overline{A}$ = mean concentration
$a' = \sqrt{\overline{a^2}}$ = root-mean-square concentration fluctuation
D = diffusivity, molecular
f = friction factor, Fanning
$f(r_x)$ = normalized correlation
F = fraction conversion
I_s = intensity of segregation
k = wave number, specific reaction rate constant
k_0 = lower wave number velocity cutoff
$k_{0,s}$ = lower wave number scalar cutoff
L_f = macroscale
L_s = scalar macroscale
n = stoichiometric coefficient
$N_{Sc} = \nu/D$ = Schmidt number
r_0 = characteristic distance
t = time
T = development time
$\overline{U}_i$ = mean velocity in the i^{th} direction
$u_i' = \sqrt{u_i^2}$ = root-mean-square velocity component in the i^{th} direction
U^* = friction velocity
x, y, z = coordinates

Greek Letters

β = stoichiometric ratio
γ = rate of strain
ϵ = turbulent energy dissipation
λ = microscale
ν = kinematic viscosity or momentum diffusivity
π = 3.1416 . . .
τ = time constant of mixing
$\varphi(k)$ = one-dimensional spectrum

Subscripts

0 = initial
s = scalar
x = axial
y, z = other directions

LITERATURE CITED

Ajmera, P. V., "Chemical Reactions and Turbulent Mixing," Ph.D. dissertation, Carnegie-Mellon Univ., Pittsburgh, Pa. (1969).

Batchelor, G. K., "Small-Scale Variation of Convected Quantities like Temperature in Turbulent Fluid," *J. Fluid Mech.*, **5**, 113 (1959).

Brodkey, R. S., "Turbulent Motion and Mixing in a Pipe," *AIChE J.*, **12**, 403 (1966).

———, "Mixing in Turbulent Fields," in *Turbulence in Mixing Operations*, R. S. Brodkey, ed., Chapt. II, Academic Press, New York (1975).
———, M. F. Cohen, Capt. J. S. Knox, G. L. McKee, K. N. MeKelvey, M. A. Rao, S. Zakanycz, and H.-n. Yieh, "Turbulence Measurements in Shear Flow Liquid Systems," Proc. Symp. Turbulence Measurements in Liquids, Dept. Ch. E., Univ. of Missouri-Rolla (1971).
Corrsin, S., "The Isotropic Turbulent Mixer: Part II. Arbitrary Schmidt Number," *AIChE J.*, **10**, 870 (1964).
Gegner, J. P., and R. S. Brodkey, "Dye Injection at the Centerline of a Pipe," *ibid.*, **12**, 817 (1966).
Gibson, C. H., and W. H. Schwarz, "Detection of Conductivity Fluctuations in a Turbulent Flow Field," *J. Fluid Mech.*, **16**, 357 (1963); "The Universal Equilibrium Spectra of Turbulent Velocity and Scalar Fields," *ibid.*, 365.
Grant, H. L., B. A. Hugehes, W. M. Vogel, and A. Moilliet, "The Spectrum of Temperature Fluctuations in Turbulent Flow," *ibid.*, **34**, 423 (1968).
Harris, I. J., and R. D. Srivastava, "The Simulation of Single Phase Tubular Reactors with Incomplete Reactant Mixing," *Can. J. Chem. Eng.*, **46**, 66 (1968).
Hinze, J. O., "Turbulence," pp. 237-8, McGraw-Hill, New York (1969).
Kattan, A., and R. J. Adler, "A Stochastic Mixing Model for Homogeneous, Turbulent, Tubular Reactors," *AIChE J.*, **13**, 580 (1967).
Keeler, R. N., L. E. Petersen, and J. M. Prausnitz, "Mixing and Chemical Reaction in Turbulent Flow Reactors," *ibid.*, **11**, 221 (1965).
Lee, J., "Turbulent Motion and Mixing," Ph.D. dissertation, The Ohio State Univ., Columbus (1962).
———, and R. S. Brodkey, "Light Probe for the Measurement of Turbulent Concentration Fluctuations," *Rev. Sci. Instr.*, **34**, 1086 (1963).
———, "Turbulent Motion and Mixing in a Pipe," *AIChE J.*, **10**, 187 (1964).
Mao, K. W. and H. L. Toor "A Diffusion Model for Reactions with Turbulent Mixing," *ibid.*, **16**, 49 (1970).
———, "Second-Order Chemical Reactions with Turbulent Mixing," *Ind. Eng. Chem. Fundamentals*, **10**, 192 (1971).
McKelvey, K. N., "Turbulent Mixing with Chemical Reaction," Ph.D. dissertation, The Ohio State Univ., Columbus (1968).
Nye, J. O., and R. S. Brodkey, "The Scalar Spectrum in the Viscous-Convective Subrange," *J. Fluid Mech.*, **29**, 151 (1967a).
———, "Light Probe for Measurement of Turbulent Concentration Fluctuations," *Rev. Sci. Instr.*, **38**, 26 (1967b).
O'Brien, E. E., "Postulate of Statistical Independence for Decaying Reactants in Homogeneous Turbulence," *Phys. Fluids*, **12**, 1999 (1969).
Patterson, G. K., "Simulating Turbulent-field Mixers and Reactors, in *Turbulence in Mixing Operations*," Chapt. V, R. S. Brodkey, ed., Academic Press, New York (1975).
Rao, D. P., and I. J. Dunn, "A Monte Carlo Coalescence Model for Reaction with Dispersion in a Tubular Reactor," *Chem. Eng. Sci.*, **25**, 1275 (1970).
Rao, D. P., and L. L. Edwards, "On the Diffusion Model of Mao and Toor," *AIChE J.*, **17**, 1264 (1971).
Toor, H. L., "Mass Transfer in Dilute Turbulent and non-Turbulent Systems with Rapid Irreversible Reactions and Equal Diffusivities," *ibid.*, **8**, 70 (1962).
———, "Turbulent Mixing of Two Species With and Without Chemical Reactions," *Ind. Eng. Chem. Fundamentals*, **8**, 655 (1969).
———, "The Non-Premixed Reaction; A + B Products," in *Turbulence in Mixing Operations*, Chapt. III, R. S. Brodkey, ed., Academic Press, New York (1975).
Torrest, R. S., and W. E. Ranz, "Improved Conductivity System for Measurement of Turbulent Concentration Fluctuations," *Ind. Eng. Chem. Fundamentals*, **8**, 810 (1969).
———, "Concentration Fluctuations and Chemical Conversion Associated with Mixing in Some Turbulent Flows," *AIChE J.*, **16**, 930 (1970).
Vassilatos, G., and H. L. Toor, "Second-Order Chemical Reactions in a Nonhomogeneous Turbulent Field," *ibid.*, **11**, 666 (1965).
Zakanycz, S., "Turbulence and the Mixing of Binary Gases," Ph.D. dissertation, The Ohio State Univ., Columbus (1971).
Yieh, H.-n., "Turbulent Mixing with Chemical Reaction," Ph.D. dissertation, The Ohio State Univ., Columbus (1970).

Manuscript received April 30, 1975; revision received August 13, and accepted August 14, 1975.

Electroosmosis and Electrolyte Conductance in Charged Microcapillaries

Interactions between the electrostatic double layer and transport rates in long capillary pores were investigated experimentally. Track-etched mica sheets with extremely narrow pore size distribution and large length-to-radius ratio were used as model membranes to examine the electrokinetic phenomena enhanced conduction and electroosmosis as a function of pore size and electrolyte (potassium chloride) concentration. Of experimental significance was that the capillary pores were of radius comparable to or even less than the solution Debye length parameter even at moderate (10^{-4} — 10^{-3} M) electrolyte concentrations. Heparin, a negatively charged polyelectrolyte, was adsorbed to the pore wall to augment electrostatic effects. The data were compared with numerical calculations based on a diffuse double-layer model, and the unknown pore wall charge densities were computed for each experiment. The results show that the classical analysis is somehow deficient and also that adsorption of the potential determining ion (heparin) is dependent on electrostatic potential at the pore wall.

WEI-HU KOH
and
JOHN L. ANDERSON
School of Chemical Engineering
Cornell University
Ithaca, New York 14853